Metabolomics (2010) 6:96–108
DOI 10.1007/s11306-009-0180-4

ORIGINAL ARTICLE

^{1}H NMR and GC-MS metabolic fingerprinting of developmental stages of *Rhizoctonia solani* sclerotia

K. A. Aliferis · S. Jabaji

Received: 3 April 2009 / Accepted: 1 September 2009 / Published online: 17 September 2009

Abstract *Rhizoctonia solani* AG-3 is a soilborne plant pathogen that forms resting vegetative structures called sclerotia. These compact structures are crucial to the pathogen's survival and pathogenesis. The metabolic changes occurring during sclerotia development were monitored using proton nuclear magnetic resonance (^{1}H NMR) spectroscopy and gas chromatography–mass spectrometry (GC-MS). The validation, discrimination, and the establishment of correlative relationships between metabolite signals were performed by principal component analysis (PCA) and partial least squares-discriminant analysis (PLS-DA). The results of the analyses suggested that out of the 116 compounds that were simultaneously analyzed and compared using GC-MS, α-α-trehalose, D-glucose, 9-(*Z*)-octadecenoic and 9,12-octadecadienoic acids, xylitol, and glucitol were key metabolites that were highly dependent on the developmental stage of the sclerotia contributing to their discrimination and classification. Furthermore, the application of ^{1}H NMR and GC-MS metabolic fingerprinting on the same biological sample provided complementary information illustrating the value of this integrated approach in the study of metabolic changes in fungal structures.

Keywords Biomarkers · Metabolites · Metabolomics · Plant pathogen · Black scurf · Potato

Electronic supplementary material The online version of this article (doi:10.1007/s11306-009-0180-4) contains supplementary material, which is available to authorized users.

K. A. Aliferis · S. Jabaji (✉)
Department of Plant Science, McGill University,
21111 Lakeshore Road, Sainte-Anne-de-Bellevue,
QC H9X 3V9, Canada
e-mail: suha.jabaji@mcgill.ca

1 Introduction

The fungus *Rhizoctonia solani* Kühn complex is a taxonomic entity composed of morphologically similar groups that share similar characteristics, multinucleate cells, production of sclerotia, and lack of conidia (Parmeter and Whitney 1970). The identification of *R. solani* isolates is based on the ability of their hyphae to anastomose (Carling 1996), and currently, there are 13 known anastomosis groups (AGs) of *R. solani* (Carling et al. 2002). Rhizoctonia disease of potato, caused by AG-3 isolates of *R. solani* is considered one of the most important fungal disease in potato fields and in certified seed production world-wide (Carling et al. 1989). The disease is characterized by the presence of cankers on the sprouts, stems and stolons and the formation of black sclerotia (black scurf) on the surface of potato tubers (Banville et al. 1996). Sclerotia of *R. solani* are compact bodies of aggregated melanized hyphae that help the pathogen to survive under unfavourable conditions for long periods due to their high resistance to chemical and biological degradation (Sumner 1996). Their formation and differentiation is triggered by oxidative stress or their thiol redox state (Georgiou and Petropoulou 2001; Patsoukis and Georgiou 2007).

Tuber-borne sclerotia are considered the most important source of inoculum for the next season, especially if potatoes are grown continuously (Sumner 1996). Complete eradication of tuber-borne sclerotia has never been achieved, while various control measures, including integrated control has reduced the incidence of the disease but not completely eradicated it (Jager et al. 1991; Secor and Gudmestad 1999; Van den Boogert and Luttikholt 2004). Comprehensive studies focusing on the physiology and chemical composition of *R. solani* sclerotia would provide useful information that could be exploited in the implementation of effective

disease control measures. Generally, studies on chemical composition of sclerotial fungi have shown that carbohydrates, proteins, lipids, fatty and amino acids, melanin-like pigments, and β-carotene are the main components (Chet and Henis 1975; Huang 1983; Abo Ellil 1999; Zervoudakis et al. 2003; Lucini et al. 2006). Despite these findings, there are no in-depth studies on the chemical composition of *R. solani* sclerotia considering that these bodies represent a key element in *R. solani* survival strategy. Earlier studies had focused on the partial characterization of phytotoxins, mainly 2-phenylacetate (syn. phenylacetic acid, PAA) and its derivatives from hyphae of *R. solani* and their role in pathogenicity (Aoki et al. 1963; Mandava et al. 1980; Iacobellis and DeVay 1987; Siddiqui and Shaukat 2005).

Based on the advances in analytical instruments and the development of specific software for the analysis of vast amounts of data, metabonomics and metabolomics have emerged within functional genomics as the fields with wide range of applications for metabolic analysis of biological systems (for review: Krishnan et al. 2005; Dunn 2008). Central to these approaches is the application of a variety of robust analytical platforms such as, nuclear magnetic resonance spectroscopy (NMR) (Ratcliffe and Shachar-Hill 2001; Ott et al. 2003; Ward et al. 2003; Aliferis and Chrysayi-Tokousbalides 2006) and mass spectrometry (MS) (Fiehn et al. 2000; Castrillo et al. 2003; Smedsgaard and Nielsen 2004; Desbrosses et al. 2005; Allwood et al. 2008; Takahashi et al. 2008). In spite of the importance of fungal metabolites, thorough assessment of their diverse metabolic landscape using metabolomic approaches is still in its infancy and has not been fully exploited. Global metabolite analysis for drug discovery, mycotoxin characterization and taxonomy of industrially and medically important yeast, yeast-like fungi and selected filamentous fungi is limited to few studies in which a variety of analytical platforms such as electrospray MS (Smedsgaard and Nielsen 2004), ^{1}H NMR (Forgue et al. 2006; Sorrell et al. 2006), GC-MS (Mas et al. 2007) or GCxGC-TOF MS (Mohler et al. 2007) were applied.

The objective of this study was to apply metabolic fingerprinting approaches for the study of the metabolic changes that occur in sclerotia of *R. solani* AG3 of different developmental stages. We have used both ^{1}H NMR spectroscopy and GC-MS coupled with robust multivariate analyses to monitor metabolic changes during sclerotia development, classify and discriminate them according to their developmental stage, and detect biomarkers. Additionally, the correlation between data obtained from ^{1}H NMR and GC-MS was investigated. Our strategy provided new insight into the complementariness and the potential of NMR and GC-MS as global metabolite fingerprinting analytical technologies for the study of fungal structures.

2 Materials and methods

2.1 Chemicals and reagents

Deuterium oxide 99.9% (D_2O) containing 0.05% trimethylsilyl-2,2,3,3-d_4-propionic acid sodium salt (TSP), pyridine 99.8%, methoxylamine hydrochloride 98%, and *N*-methyl-*N*-(trimethyl-silyl)trifluoroacetamide (MSTFA) were purchased from Sigma–Aldrich Ltd. (Oakville, ON, Canada), and analytical standards from Restek Corporation (Bellefonte, PA, USA). Ethyl acetate and methanol (99.9%) were purchased from Fisher Scientific Company (Ottawa, ON, Canada).

2.2 Fungus and culture conditions

Starter cultures of a highly pathogenic isolate of *Rhizoctonia solani* AG3P (RS 114), obtained from M. Cubeta (North Carolina University, USA) were maintained on oat kernels at 4°C. Agar plugs from starter cultures were placed on the surface of culture plates (9 cm in diameter) containing potato dextrose agar (PDA; Becton–Dickinson Microbiology Systems, Sparks, MD) and covered with cellophane membrane (500 PUT; UCB, North Augusta, USA), and grown at 24°C in the dark. Sclerotial initials appeared after 4 days and mature sclerotia were harvested using forceps at 8, 16 and 24 days of growth. There were five replicate culture plates per developmental stage. Each replicate constituted of 50 mg (fresh weight) of sclerotia collected from a single culture plate. Samples were pulverized into fine powder in porcelain mortar in liquid nitrogen and immediately lyophilized in screw thread autosampler vials (2 ml) for 24 h and kept in −80°C until further analyses.

2.3 Chemical analyses and data pre-processing

2.3.1 Metabolic fingerprinting of sclerotial extracts using ^{1}H nuclear magnetic resonance spectroscopy

Lyophilized samples were extracted in D_2O (1.0 ml) for 4 h under continuous agitation (120 rpm) at 24°C for the extraction of polar compounds. Preparations were centrifuged at 12,000×*g* for 60 min at 4°C and the supernatants were collected and further purified by a second centrifugation at 12,000×*g* for 30 min. The NMR samples were prepared from the supernatants (0.8 ml) and were kept frozen (−80°C) in screw thread autosampler vials until the acquisition of ^{1}H NMR spectra.

The ^{1}H NMR spectra of polar sclerotial extracts were recorded using a Varian Inova 500 MHz NMR spectrometer (Varian, CA, USA) equipped with a ^{1}H{^{13}C,^{15}N} triple

resonance cold probe. A total of 256 transients of 32 K data points were acquired per sample with a 90° pulse angle, 2 s acquisition time, and 2 s recycle delay with presaturation of H_2O during the recycle delay. For each developmental stage, five biological replications were performed.

Spectra were Fourier transformed, the phase and the baseline were automatically corrected (Aliferis and Chrysayi-Tokousbalides 2006), using MestReC software (v.461, Mestrelab Research, Santiago de Compostela, Spain). Prior to statistical analyses spectra were aligned as proposed by Defernez and Colquhoun (2003) using MestReC software. Offsets of chemical shifts were corrected based on the reference signal of TSP (0.00 ppm). Additionally, the spectral regions δ 4.5-5.1 were removed to eliminate the effects of imperfect water suppression. In order to reduce the size of the data without a concomitant loss of spectra resolution, binning of spectra using a bin width of 0.001 ppm was performed (Mnova Suite; v.5.3.2, Mestrelab Research, Santiago de Compostela, Spain). Spectra were then exported as ".txt" files to MS Excel® and normalized prior to pattern recognition analysis to the total intensity. NMR data matrices were composed of 15 observations (rows) with 8,900 variables (columns) each.

In a final step, results from multivariate analyses of ^{1}H NMR data matrix were interpreted with those obtained from GC-MS fingerprinting. The ^{1}H NMR chemical shifts of compounds that found to be influential for the observed discrimination applying GC-MS were predicted using NMR software and databases [C+H NMR Predictor and Database v.12.01, Advanced Chemistry Development, Inc. (ACD/Labs, Toronto, Canada) the Human Metabolome Database (http://www.hmdb.ca), and the Spectral Database for Organic Compounds SDBS (http://riodb01.ibase.aist.go.jp/sdbs/cgi-bin/direct_frame_top.cgi)]. These shifts were cross-validated using results obtained from ^{1}H NMR fingerprinting analyses.

2.3.2 *Metabolic fingerprinting of sclerotial extracts using gas chromatography–mass spectrometry*

Extraction of the lyophilized sclerotial samples was performed in screw thread autosampler vials (2 ml) using 1 ml of a mixture of ethyl acetate–methanol (50:50, v/v) under continuous agitation (150 rpm) for 24 h at 24°C. Extracts were then filtered through 0.2 μm filters (Millex-FG, Millipore, MA, USA) and concentrated to complete dryness using a Speedvac® AES1010 (Savant Instruments Inc, NY, USA). For the derivatization of the samples, the method of Börner et al. (2007) with some modifications was performed in two steps: (i) a methoxylamine hydrochloride solution (20 mg/ml in pyridine) (80 μl) at 30°C for 120 min was added followed by (ii) the addition of MSTFA (80 μl) at 37°C for 90 min. Derivatized samples were kept at room temperature in the dark for 24 h prior to analyses.

Analysis of samples was performed using a Varian Saturn 2100T GC/MS/MS system (Varian, CA, USA) equipped with a CP-8400 autosampler. The ionization mode was electron ionization at 70 eV and the value of the electron multiplier voltage was 1,750 V throughout the experiment. The temperature for the ion source was set to 150°C and for the transfer line to 250°C. Full scan mass spectra were acquired from 40 to 650 m/z at 1 scans s^{-1} rate with a 10.0-min solvent delay. A Varian CP-Sil 8 CB capillary column (30 m, i.d. 0.25 μm) was used with helium flow of 1 ml min^{-1}. For the injection of samples (1 μl) standard column mode with a split ratio of 10 was used at an injection temperature of 230°C. The initial temperature of the oven was set at 70°C stable for 5 min, followed by a 5°C min^{-1} increase to 310°C, stable for 1 min. Mass calibration of the instrument was made weekly with perfluorotributylamine (PFTBA, FC-43, Varian, CA, USA). Blank samples were analyzed in order to detect possible contamination resulting from the reagents, sample preparation, or the instrument. No internal standard was used as only relative changes were studied.

Chromatogram acquisition, automated peak deconvolution and library searches were performed using the Saturn GC/MS Workstation (version 5.51, Varian, CA, USA) in combination with the automated deconvolution and identification system (AMDIS, version 2.0). Mass spectra searches were performed using the libraries of the National Institute of Standards and Technology (NIST). Additionally, on-line mass spectra searches in the Golm Metabolome Database, (http://csbdb.mpimp-golm.mpg.de/ csbdb/gmd/msri/gmd_sspq.html), the Human Metabolome Database (http://www.hmdb.ca) and the Spectral Database for Organic Compounds SDBS (http://riodb01.ibase.aist.go.jp/sdbs/cgi-bin/direct_frame_top.cgi) were performed.

Peaks corresponding to column bleeding and reagent peaks were excluded from further analyses. Total ion chromatograms were aligned and dataset composed of 116 metabolites was subjected to multivariate analyses without a prior identification of the compounds. Data were exported as ".txt" files to MS Excel® and normalized prior to pattern recognition analysis to the total peak area. In total, five biological replications were performed for each developmental stage. After multivariate analyses of spectra, selected substances were verified with commercially purchased analytical standards, whereas in cases in which a very good fit could be achieved tentative identification was performed.

2.4 ^{1}H NMR and GC-MS multivariate data analyses

Pre-processed ^{1}H NMR (15 observations with 8,900 variables each) and GC-MS (15 observations with 116

variables each) data matrices as described above were exported to SIMCA-P$^+$ 12.0 software (Umetrics, MKS Instruments Inc., Sweden) for multivariate data analyses. A free demo version of the software is available (http://www.umetrics.com/default.asp/pagename/downloads_software/c/1). Data were Pareto scaled ($1/\sqrt{SD}$) and visualized by plotting the principal components scores in which each coordinate represents an individual biological sample. For the classification and discrimination between the treatments, principal components analysis (PCA) and partial least squares-discriminant analysis (PLS-DA) were carried out. Cross validation of the developed models was performed based on the default software options and the resulting values of explained variation (R^2X and R^2Y) and predictive ability [$Q^2_{(cum)}$] were used. The detection of differences in metabolic fingerprints was based on PLS-DA and scaled PLS regression coefficients which identify variables that change when going from one group of treatments to another (Eriksson et al. 2001). Standard errors were calculated using jack-knifing which is based on the variability in the model parameters encountered in the different cross-validation cycles with 95% confidence interval (Efron and Gong 1983).

The performance of the developed models was assessed by the cumulative fraction of the total variation of the *X*'s that could be predicted by the extracted components [$Q^2_{(cum)}$] and the fraction of the sum of squares of all *X*'s and *Y*'s explained by the current component (R^2X and R^2Y). In general, values of $Q^2_{(cum)}$ over 0.5 are considered good whereas values above 0.9 are considered excellent for metabonomic experiments. In addition to SIMCA-P+, JMP v.4.1 (SAS Institute, NC, USA) was used for regression analysis of data.

3 Results and discussion

3.1 Sclerotia production

White sclerotial initials of *R. solani* were formed 4 days after inoculation of the medium and their colour progressively changed to brown and became highly pigmented as they matured. Mature sclerotia are characterized by melanin pigmentation and often associated with droplet excretion (Chet and Henis 1975). Under the described growth conditions, the total fresh weight of the sclerotia per culture plate significantly ($P \leq 0.05$) increased with developmental stage (Table 1).

Table 1 Fresh weight of scelortia of *Rhizoctonia solani* cultures expressed as mg of fresh weight per culture plate

Developmental stage (days)	Fresh weight of sclerotia (mg)
8	1593.1 ± 92.5^a
16	2458.8 ± 114.1^b
24	2896.4 ± 163.2^c

Results represent the means of five replications ± standard deviation. Means followed by the same letter are not significantly different based on Tukey's HSD test ($P \leq 0.05$)

3.2 Multivariate analyses of sclerotial composition applying ^{1}H NMR and GC-MS metabolic fingerprinting

^{1}H NMR and GC-MS metabolic fingerprinting were applied as high-throughput methods for detecting metabolic differences between sclerotia of different developmental stages. ^{1}H NMR fingerprinting overcomes the assignment problem of compounds in complex mixtures due to overlapping signals without the identification of the metabolites to be the primary task. On the other hand, the sensitivity of the GC-MS in combination with the chromatographic separation and MS databases enables the identification of compounds in complex mixtures. Representative ^{1}H NMR spectra and total ion chromatograms of crude extracts of 8, 16 and 24-day-old sclerotia of *R. solani* with annotations for selected of the detected metabolites are presented in Figs. 1 and 2, respectively.

In order to evaluate differences in the acquired ^{1}H NMR spectra and GC-MS total ion chromatograms, PCA was carried out on the pre-processed ^{1}H NMR and GC-MS data matrices for an initial evaluation of the developed models and the detection of outliers that could influence their predictive ability and trends. Examination of PCA score plots allows for identification of spectra with similar metabolic profiles which will plot close together. The PCA scores plot showed that none of the samples were outside the Hotelling T^2 95% confidence with high values of $R^2X = 0.96$ and $Q^2_{(cum)} = 0.75$ (7 principal components-*PCs*) for the ^{1}H NMR, and $R^2X = 0.96$ and $Q^2_{(cum)} = 0.74$ (5 *PCs*) for the GC-MS. A higher explained variation was observed for the GC-MS model plotting PC1 vs. PC2 (Fig. 3). Additionally, PCA models were created for each group of developmental stage in order to examine the reproducibility of the applied protocols and instrument performance. Analyses revealed tight classes for all groups with high values of explained variation for ^{1}H NMR [8 ($R^2X = 0.87$, 2 *PCs*), 16 ($R^2X = 0.84$, 2 *PCs*), and 24-day-old ($R^2X = 0.78$, 2 *PCs*) sclerotia] and for GC-MS [8 ($R^2X = 0.78$, 2 *PCs*), 16 ($R^2X = 0.88$, 2 *PCs*), and 24-day-old ($R^2X = 0.88$, 2 *PCs*) sclerotia].

PLS-DA is commonly used to detect hidden variables that focus on class separation (Eriksson et al. 2001). Thus, PLS-DA models for ^{1}H NMR and GC-MS were developed from training sets of observations of known membership class to detect the most influential metabolites for the

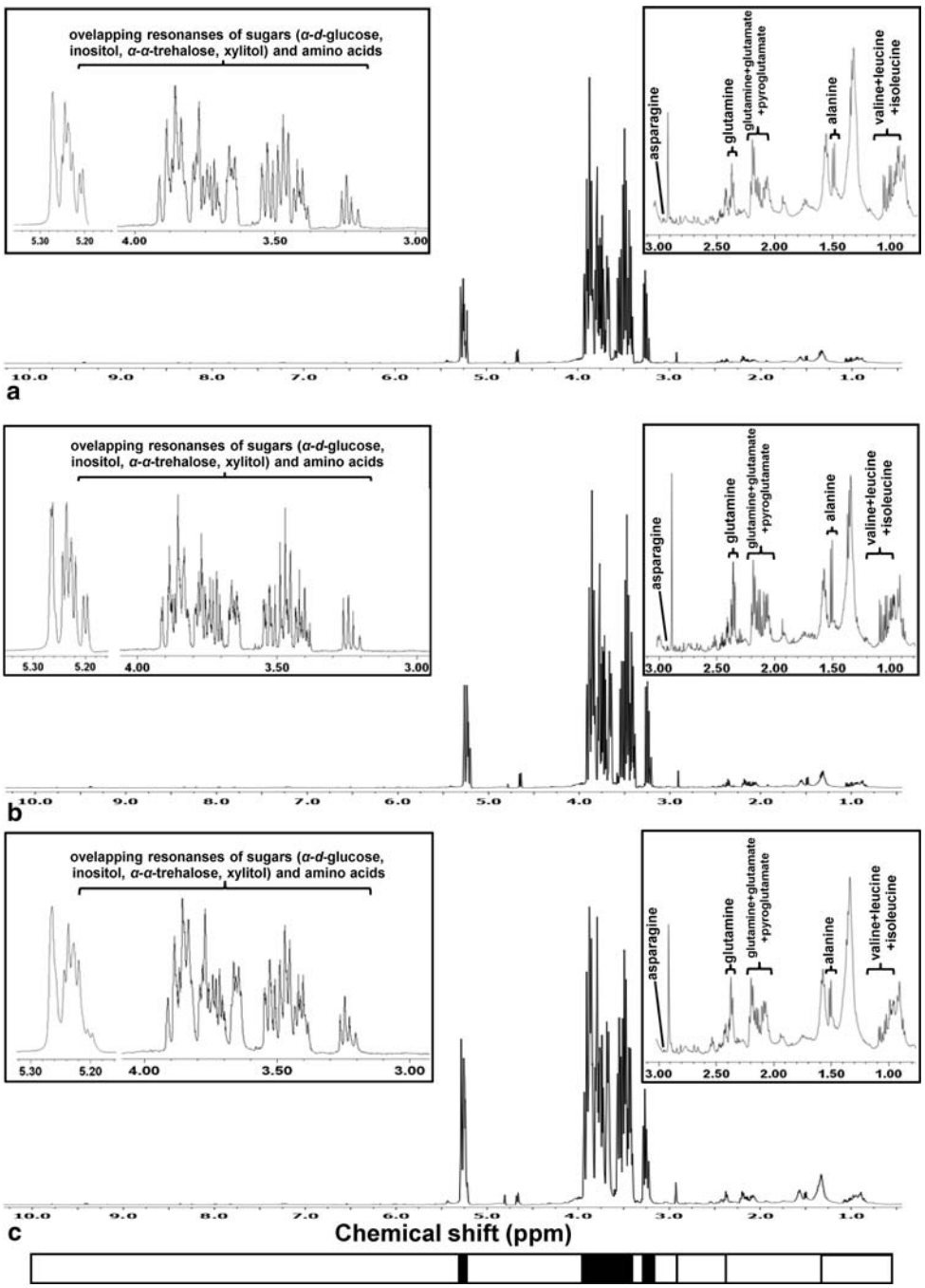

Fig. 1 Representative ^{1}H NMR spectra of crude extracts of 8 (**a**), 16 (**b**), and 24 (**c**)-day-old sclerotia of *Rhizoctonia solani* AG3. Chemical shifts (ppm) that influence the separation are indicated below the axes. Resonances are annotated according to the chemical shifts in Fig. 1s

discrimination between the different developmental stages of sclerotia (i.e., 2-time points at a time). For ^{1}H NMR models, PLS-DA PC1/PC2 score plots for all combinations of groups of developmental stages in pairs showed a strong separation with values of $Q^2_{(cum)}$ ranging from 0.89 to 0.93 (Table 2, Fig. 4) which indicates that substantial chemical changes occurred during sclerotia development. Additionally, the chemical shifts, δ 3.23–3.91 and 5.19–5.27 (ppm) significantly contributed to the separation between the different developmental stages (Table 2, Figs. 1 and 4). Compounds containing amine, hydroxy, methine, methyl, methylene, olefin, and thiol groups were influential in the observed separation, while aromatic and aldehydic compounds had no contribution as indicated by the absence of influential variables above the chemical shift δ 5.27 of the spectra (Table 2, Figs. 1 and 4).

For GC-MS, after spectra deconvolution and pre-processing, profiles of sclerotia consisted of 116 compounds were created. PLS-DA score plots for all combinations of developmental stages in pairs and cross validation analyses showed a very strong separation as indicated by the high values of $Q^2_{(cum)}$ ranging from 0.93 to 0.97 (Table 2 and

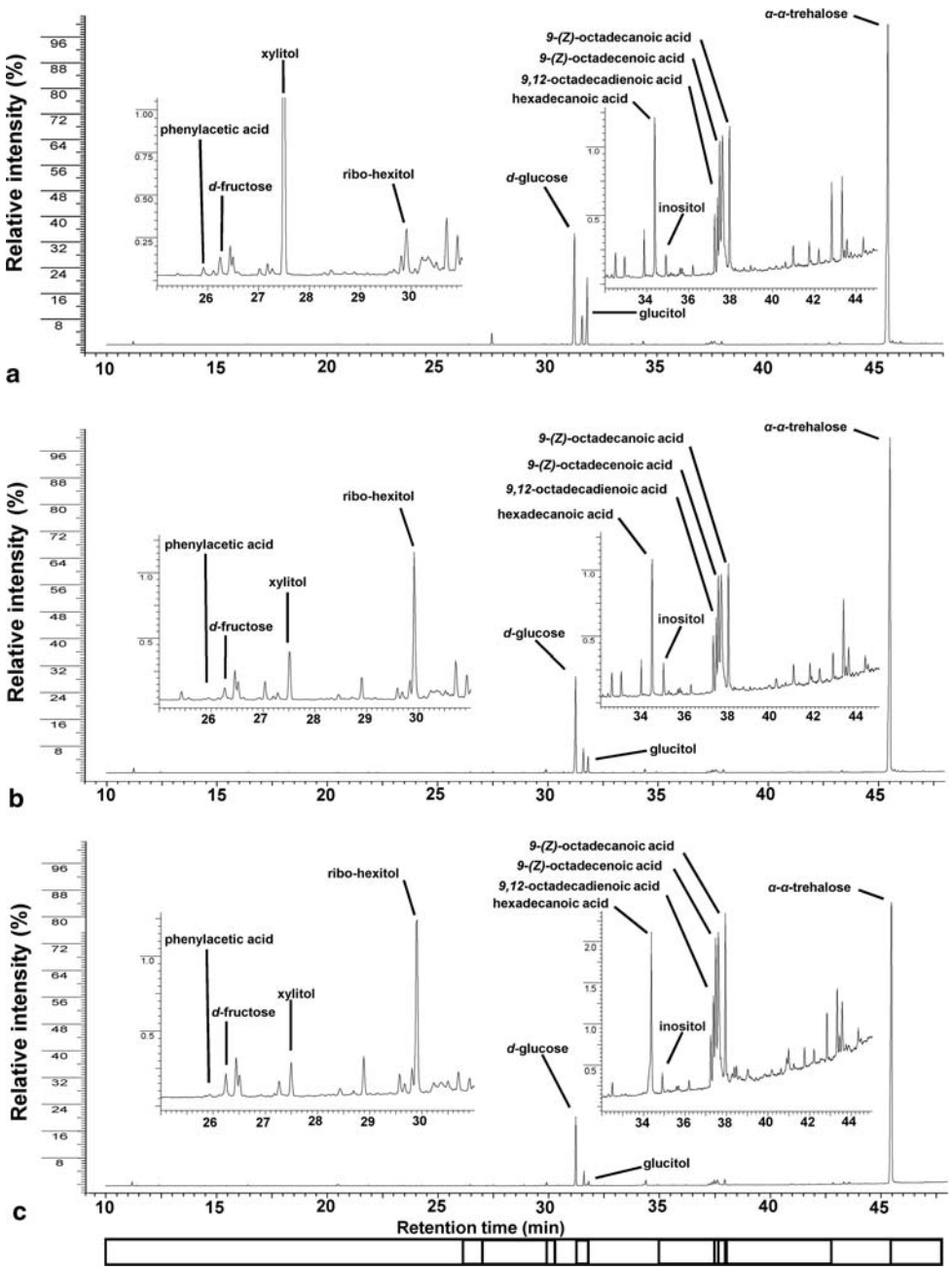

Fig. 2 Representative GC-MS total ion chromatograms of crude extracts of 8 (**a**), 16 (**b**), and 24 (**c**)-day-old sclerotia of *Rhizoctonia solani* AG3. Retention times (min) corresponding to compounds that influence the separation are indicated below the axes. Annotations of representative metabolites are displayed

Fig. 5). Significant changes in the chemical composition of sclerotia were detected using PLS regression coefficients with 95% jack-knifed confidence intervals (Fig. 6), and one-way ANOVA performing the Tukey's HSD test with 95% confidence interval (Fig. 7). Compounds whose concentration varied substantially in different developmental stages of sclerotia were further identified (Figs. 6 and 7) based on mass spectra queries. The relative concentrations of α,α-trehalose, the unsaturated fatty acids 9-(*Z*)-octadecenoic (syn. oleic acid, C18:1) and 9,12-octadecadienoic (syn. linoleic acid C18:2), D-glucose, and the sugar alcohols, xylitol and glucitol (syn. sorbitol) significantly varied with sclerotial age (Figs. 6 and 7).

In total, thirty-nine compounds were identified; six amino acids (Fig. 7b), eight carboxylic acids (Fig. 7g), one polysaccharide (Fig. 7a), six monosaccharides (Fig. 7a, e), four sugar alcohols (Fig. 7f), two unsaturated (Fig. 7c) and four saturated fatty acids (Fig. 7d), and eight compounds belonging to several chemical groups (Fig. 7h). These metabolites represent more than 96.0% of the relative composition of each metabolic profile. From the remaining metabolites, 43 were completely unknown. The analysis of

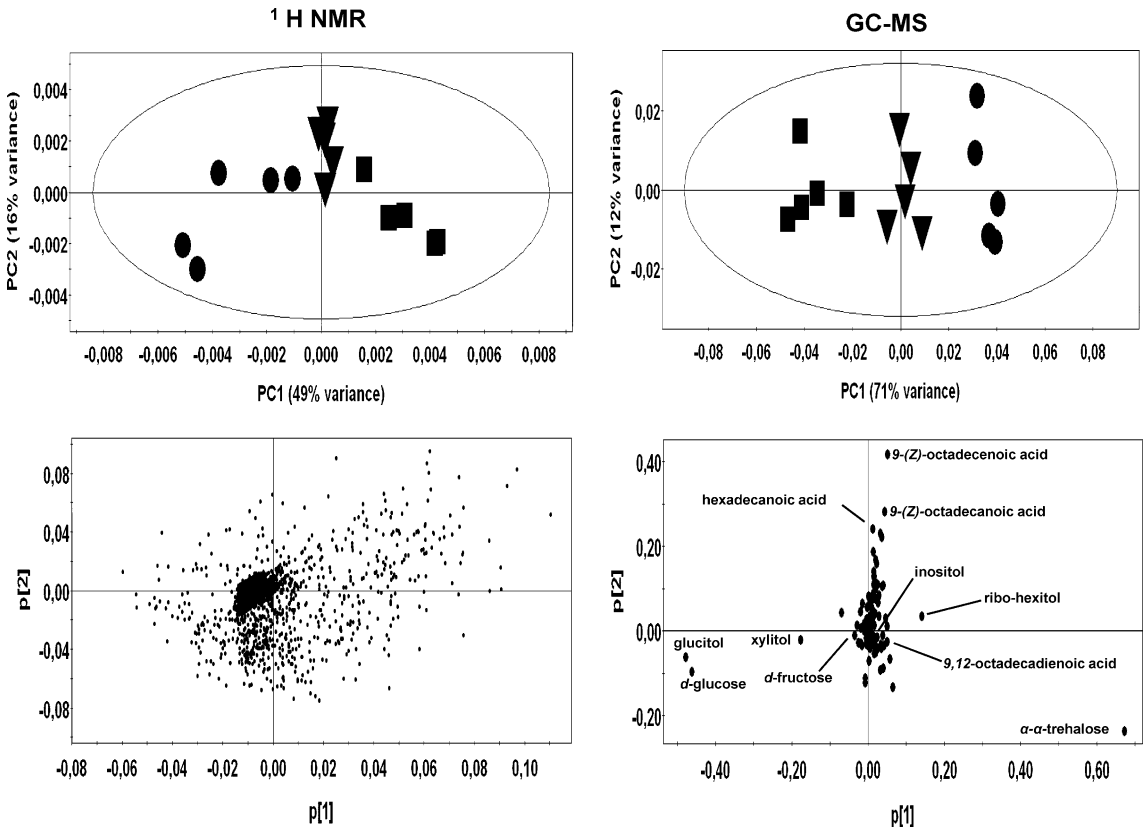

Fig. 3 PCA PC1/PC2 score plots with corresponding p_1/p_2 loading plots of ^{1}H NMR and GC-MS total ion chromatogram data matrices of crude *Rhizoctonia solani* AG3 sclerotial extracts. For each principal component identified metabolites with the higher loadings are indexed in the GC-MS loading plot. The ellipse represents the Hotelling T^2 with 95% confidence interval [8 (*filled square*), 16 (*filled inverted triangle*), and 24 (*filled circle*)-day-old sclerotia]

Table 2 Cross validation analysis in which pair of sclerotia groups were compared performing partial least squares-discriminant analysis (PLS-DA) applying ^{1}H NMR and GC-MS metabolic fingerprinting

Analytical platform	Compared groups of sclerotia (age in days)	Parameters[a]				Influential variables[b]
		PCs	R^2X	R^2Y	$Q^2_{(cum)}$	
^{1}H NMR						Shift ranges (δ ppm)
	8/16	3	0.78	0.98	0.89	1.30–1.32, 2.34–2.36, 2.91, 3.20, 3.23–3.26, 3.38–3.59, 3.63–3.79, 3.81–3.91, 5.19–5.27
	8/24	3	0.73	0.97	0.91	1.30–1.31, 2.35, 3.23–3.55, 3.63–3.89, 3.90–3.92, 5.19–5.21, 5.22–5.27
	16/24	3	0.57	0.98	0.76	2.90, 3.23–3.26, 3.38–3.91, 5.19–5.27
GC-MS						Metabolites/retention times (RT minutes)
	8/16	2	0.78	0.98	0.93	Cmpd[c] RT 30.216, glucitol, D-glucose, inositol, 9-(*Z*)-octadecenoic acid, 9,12-octadecadienoic acid, α-α-trehalose, xylitol
	8/24	2	0.89	0.97	0.97	Glucitol, D-glucose, inositol, 9,12-octadecadienoic acid, α-α-trehalose, xylitol
	16/24	2	0.88	0.93	0.93	Cmpd RT 37.238, Cmpd RT 42.834, *d*-fructose, glucitol, D-glucose, inositol, 9,12-octadecadienoic acid, *d*-ribo-hexitol, α-α-trehalose

The ^{1}H NMR spectra regions and metabolites analyzed by GC-MS responsible for the discrimination are displayed

[a] *PCs*; principal components, $Q^2_{(cum)}$; the cumulative fraction of the total variation of the *X's* that can be predicted by the extracted components, R^2X and R^2Y; the fraction of the sum of squares of all *X's* and *Y's*, respectively, explained by the current component

[b] The detection of the influential variables for the observed separation was based on scaled and centered PLS regression coefficients (CoeffCS) with 95% jack-knifed confidence intervals

[c] *Cmpd*; compound

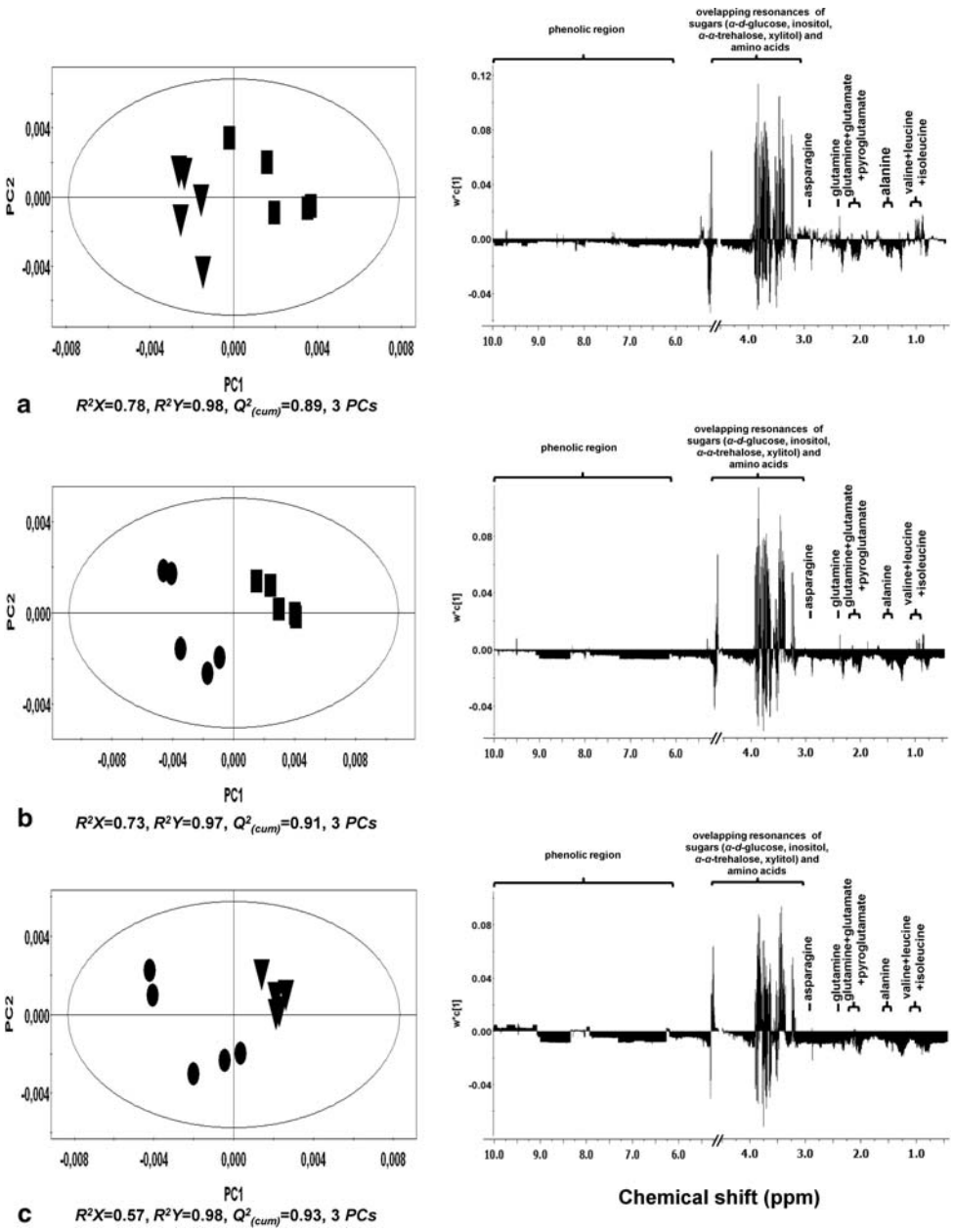

Fig. 4 PLS-DA PC1/PC2 score plots with corresponding w*c[1] loading plots for all developmental stages in pairs performing ^{1}H NMR fingerprinting. Resonances are annotated according to the chemical shifts in Fig. 1s. The ellipse represents the Hotelling T^2 with 95% confidence interval [8 (*filled square*), 16 (*filled inverted triangle*), and 24 (*filled circle*)-day-old sclerotia]

blank samples revealed only the presence of artifacts resulting from column bleeding. Regarding the on-line mass spectral libraries, only the Golm Metabolome Database gave satisfactory results that were comparable to those of NIST libraries whereas inadequate results were obtained from searches performed using the remaining data mining libraries.

3.3 Physiological significance of metabolic changes in sclerotia of different developmental stages

Significant metabolic changes occurring during the development of sclerotia were analyzed by GC-MS fingerprinting (Figs. 6, 7). The relative composition of α,α-trehalose (Fig. 7a) and unsaturated fatty acids (Fig. 7c) significantly increased with the developmental stage. Trehalose is a well-known storage carbohydrate in eukaryotic cellls (Argüelles 2000). The analysis of the sclerotial extracts clearly showed that α-α-trehalose is the most abundant compound with an increase in its relative content by 12.4% in 24-day-old sclerotia as compared to 8-day-old sclerotia (Fig. 7a). The role of trehalose in the adaptation to desiccation tolerance or anhydrobiosis of cell membranes of eukaryotes including fungi is well established (Iturriaga 2008). This unique property is due to the α,α-(1 → 1) glycosidic linkage of the molecule which is effective against membrane damage and is known to preserve cell membrane integrity (Albertorio et al. 2007; Christensen et al. 2007). Based on these findings,

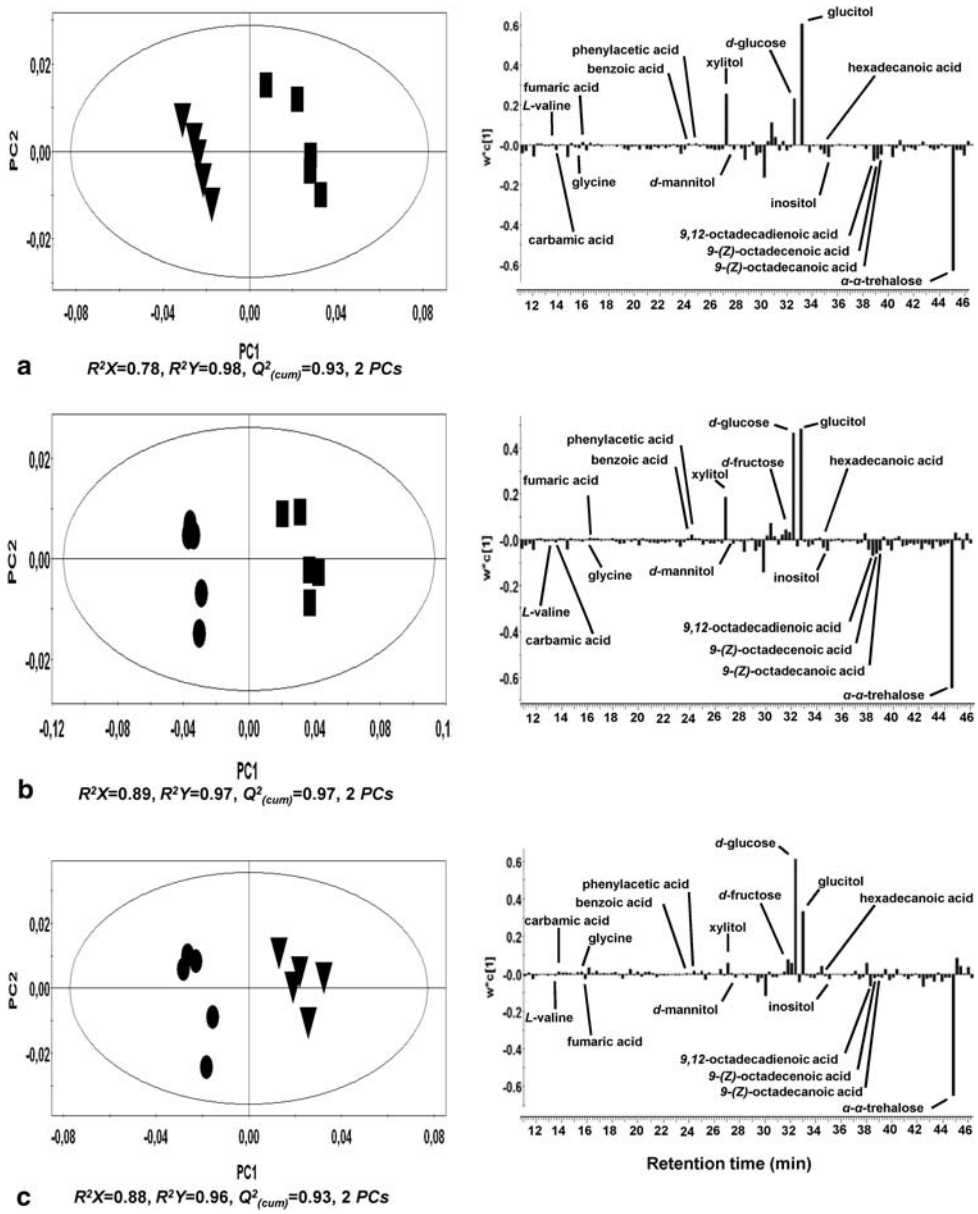

Fig. 5 PLS-DA PC1/PC2 score plots with corresponding w*c[1] loading plots for all developmental stages in pairs performing GC-MS fingerprinting. Representative metabolites are displayed. The ellipse represents the Hotelling T^2 with 95% confidence interval [8 (*filled square*), 16 (*filled inverted triangle*), and 24 (*filled circle*)-day-old sclerotia]

this disaccharide is likely to play a key role in sclerotial physiology and survival, in addition to its function as the major endogenous storage carbohydrate in sclerotial fungi (Chet and Henis 1975). Furthermore, the role of trehalose in fungal pathogenesis has been demonstrated in the causal agent of rice blast disease, *Magnaporthe grisea* (Foster et al. 2003). Thus, strategies targeting the biosynthetic pathway of trehalose should be considered in the context of developing new crop protection strategies against *R. solani*.

Parallel to the increase in trehalose content, a progressive increase in the total unsaturated fatty acid content of sclerotia was also observed (Figs. 6 and 7c, d). PLS regression coefficients analysis showed that the unsaturated 9-(*Z*)-octadecenoic and 9,12 octadecadienoic acids largely differed with the developmental stage. Fatty acids in fungi play a significant role in mycotoxin biosynthesis, sporulation, and differentiation processes (Noverr and Huffnagle 2004; Yu and Keller 2005). In *Rhizoctonia* species, palmitic, oleic and linoleic acids are the major fatty acids, comprising 94–98% of the whole fatty acid content (Priyatmojo et al. 2002). Among them, oleic acid and linoleic were abundant in sclerotia of *R. solani* with a shift in synthesis pattern and composition that varied with age (Gottlieb and Van Etten 1966). These findings are in agreement with the present study.

In contrast to trehalose and unsaturated fatty acids, a decrease in the relative composition of sugar alcohols, xylitol and glucitol with the developmental stage was

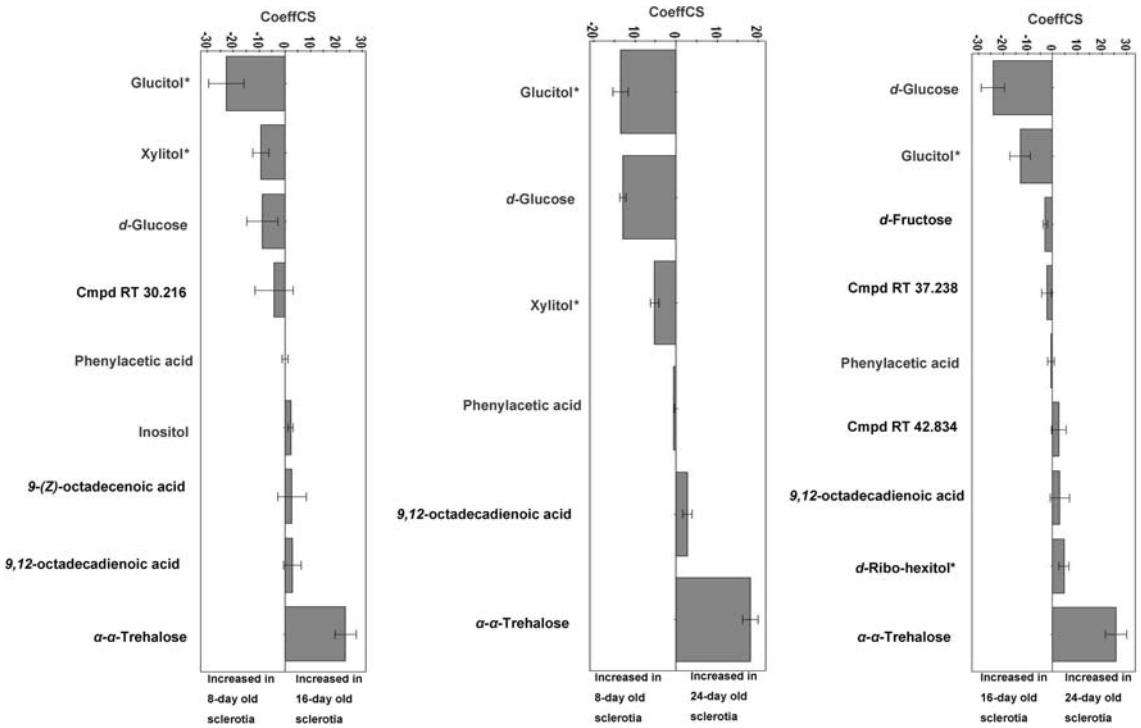

Fig. 6 PLS coefficient plots for GC-MS data matrices with values of scaled and centered PLS regression coefficients (CoeffCS) for the selected *Y* variables. The most influential variables to the observed separation are displayed with 95% jack-knifed confidence intervals. Phenylacetic acid was included in the plot because it is a common metabolite implicated in *Rhizoctonia solani* pathogenesis. Compounds marked with an asterisk were tentatively identified

observed (Figs. 6 and 7f). Xylitol is an intermediate product of glycolysis of pentoses (i.e., pentose and glucoranate interconversions, http://www.genome.jp/dbget-bin/show_pathway?ko00040+C00379). The significant decrease in xylitol in 16 and 24 day compared to 8-day-old sclerotia could be an indication of progressive slowdown of glycolysis. Glucitol has been reported as the metabolic intermediate of glucose in some fungi (Manners et al. 1984). Although no direct evidence is available in our study, it is plausible to suggest that decreased levels of glucitol is associated with the decreased levels of the precursor D-glucose in sclerotia with time.

On the other hand, the decreased levels of D-glucose with time could also be related to the increase in trehalose. This is based on the observation that the ratio of α-α-trehalose to D-glucose was progressively increased with time from 3.32 in 8-day-old sclerotia to 5.57 in 24-day-old sclerotia in this study (Fig. 7a), and the fact that glucose has been identified as the precursor in the biosynthetic pathway for trehalose (Cabib and Leloir 1958; Avonce et al. 2006). Taken together, it can be concluded that the disaccharide α-α-trehalose is the favourable form of carbon assimilation in the sclerotia of *R. solani* under the specified conditions.

PAA is an intermediate product of phenylalanine metabolism (http://www.genome.jp/dbget-bin/show_pathway?ko00360+C00642) and has been widely implicated in the pathogenesis of *R. solani* (Aoki et al. 1963; Frank and Francis 1976; Mandava et al. 1980; Siddiqui and Shaukat 2005). In all of these studies, PAA was either extracted from mycelia or from culture filtrates but not from sclerotia. Our results represent the first report on the presence of PAA in sclerotia of *R. solani*. Interestingly, metabolomic analysis revealed no significant changes in the levels of PAA during sclerotia development (Figs. 6 and 7g). This finding, suggests that there is no direct relation between sclerotia development and PAA content, and therefore this compound does not play a major role in the physiological process under our described conditions.

Interestingly, the relative content of the remaining identified compounds significantly changed in sclerotia of different developmental stages mainly due to the increase in the relative concentration of ribo-hexitol (Fig. 7h). Additionally, there was a marked increase of compounds corresponding to retention times (RT) 30.078, 30.216, 37.238 (alkane), and 42.834 min that could not be identified (Fig. 6).

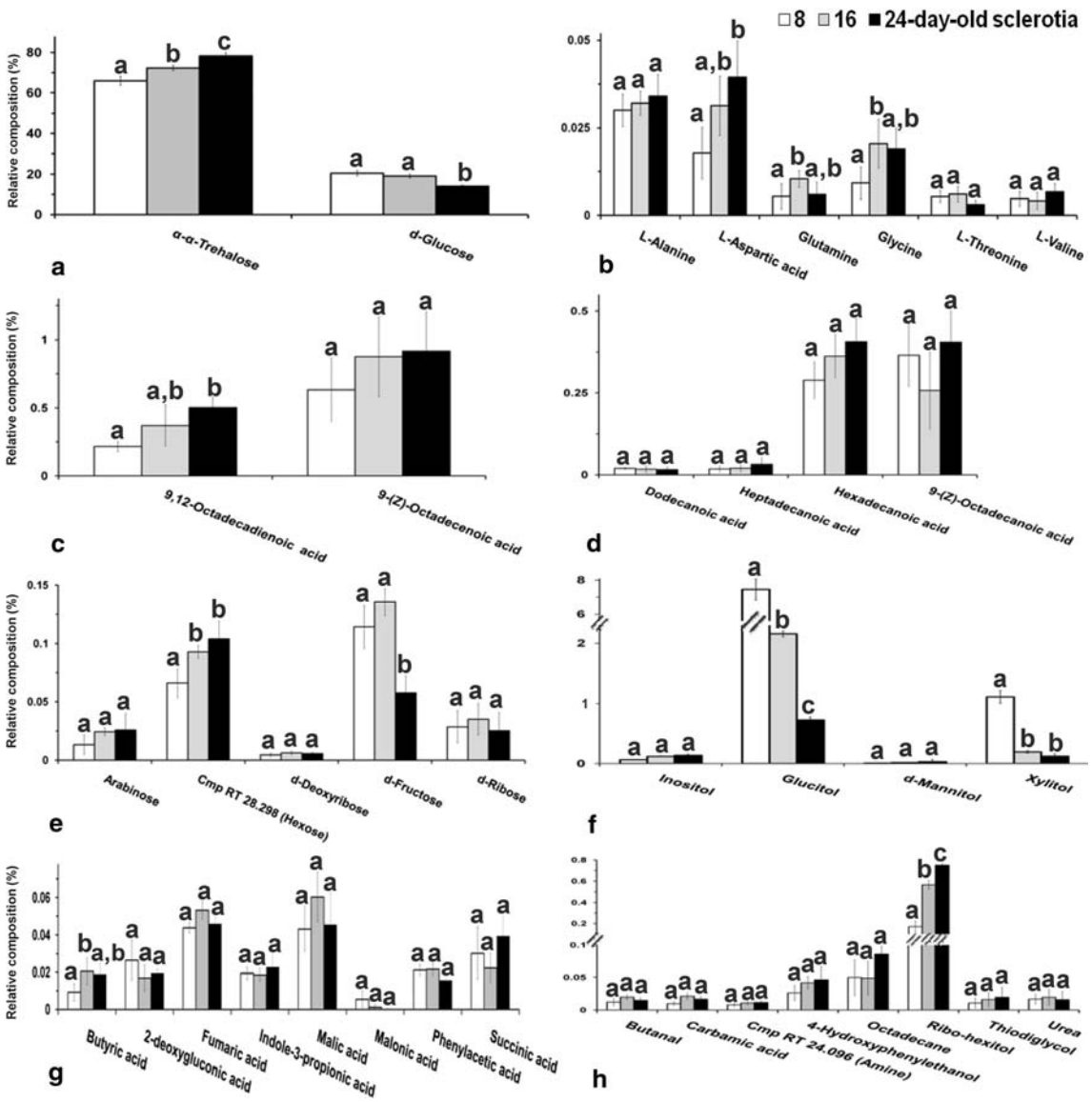

Fig. 7 Relative chemical composition of extracts of 8, 16, and 24-day-old *Rhizoctonia solani* sclerotia in α-α-trehalose (polysaccharide) and D-glucose (monosaccharide) (**a**), amino acids (**b**), unsaturated (**c**) and saturated fatty acids (**d**), monosaccharides (**e**), sugar alcohols (**f**), carboxylic acids (**g**), and compounds belonging to several chemical groups (**h**). Samples were analyzed with GC-MS. Each bar represents the mean of five replications and standard deviations are plotted as vertical bars. Same letters designate no significant differences performing Tukey's HSD test ($P \leq 0.05$)

3.4 Interpretation of results from ^{1}H NMR and GC-MS metabolic fingerprinting

The assignment of ^{1}H NMR chemical shifts in complex mixtures to the corresponding compounds is a challenging task in metabolomics studies. In our study, we took advantage of both ^{1}H NMR and GC-MS approaches in the analysis of the same biological sample in combination with the use of specific software and databases. Using the ACD/C+H NMR Predictor and Database v.12.01 and on-line databases, chemical shifts of metabolites influential for the discrimination between the different developmental stages (Table 2) could be satisfactorily correlated to shifts of the influential metabolites identified with GC-MS (Fig. 1s). These results are indicative of the complementariness of the two analytical platforms for metabolomic studies and the validity of the analytical methodologies that were followed.

4 Concluding remarks

The application of ^{1}H NMR spectroscopy and GC-MS metabolic fingerprinting approaches using the same biological material allowed a direct comparative analysis

between the platforms. Data generated from robust statistical analyses indicated that a substantial number of significantly correlating metabolite signals are dependent on the developmental stage of the sclerotia and are potentially reliable biomarkers in the study of sclerotial development.

Although the applied protocols differed, results from ^{1}H NMR and GC-MS metabolomic analyses were qualitatively similar suggesting that both platforms complement each other in providing richer information than that achievable by each method alone, and can be applied for high-throughput metabolic fingerprinting of similar biological systems, depending on the aim of a given study and the available instrumentation.

Acknowledgments The authors thank Dr. W.D. Marshall for providing access to GC-MS instrument and Dr. T. Sprules, the Quebec/Eastern Canada High Field NMR Facility, for her assistance with the NMR spectra. Funding for this was provided by the Natural Sciences and Engineering Research Council of Canada (NSERC) discovery Grants and a Post-doctoral fellowship to Dr. K. Aliferis funded by the Fonds Québécois de la Recherche sur la Nature et les Technologies (FQRNT) and McGill University.

References

Abo Ellil, A. H. A. (1999). Oxidative stress in relation to lipid peroxidation, sclerotial development and melanin production by *Sclerotium rolfsii*. *Journal of Phytopathology, 147*, 561–566.

Albertorio, F., Chapa, V. A., Chen, X., Diaz, A. J., & Cremer, P. S. (2007). The α, α-(1 → 1) linkage of trehalose is key to anhydrobiotic preservation. *Journal of the American Chemical Society, 129*, 10567–10574.

Aliferis, K. A., & Chrysayi-Tokousbalides, M. (2006). Metabonomic strategy for the investigation of the mode of action of the phytotoxin (5*S*, 8*R*, 13*S*, 16*R*)-(–)-pyrenophorol using ^{1}H nuclear magnetic resonance fingerprinting. *Journal of Agricultural and Food Chemistry, 54*, 1687–1692.

Allwood, J. W., Ellis, D. I., & Goodacre, R. (2008). Metabolomic technologies and their application to the study of plants and plant–host interactions. *Physiologia Plantarum, 132*, 117–135.

Aoki, H., Sassa, T., & Tamura, T. (1963). Phytotoxic metabolites of *Rhizoctonia solani*. *Nature, 200*, 575.

Argüelles, J. C. (2000). Physiological roles of trehalose in bacteria and yeasts: A comparative analysis. *Archives of Microbiology, 174*, 217–224.

Avonce, N., Mendoza-Vargas, A., Morett, E., & Iturriaga, G. (2006). Insights on the evolution of trehalose biosynthesis. *BMC Evolutionary Biology, 6*, 109.

Banville, G. J., Carling, D. E., & Otrysko, B. E. (1996). Rhizoctonia disease in potato reaction. In S. Sneh, S. Jabaji-Hare, S. Neate, & G. Dijst (Eds.), *Rhizoctonia species: Taxonomy, molecular biology, ecology, pathology, and disease control* (pp. 321–330). Dordrecht: Kluwer Academic Publishers.

Börner, J., Buchinger, S., & Schomburg, D. (2007). A high-throughput method for microbial metabolome analysis using gas chromatography/mass spectrometry. *Analytical Biochemistry, 367*, 143–151.

Cabib, E., & Leloir, L. F. (1958). The biosynthesis of trehalose phosphate. *The Journal of Biological Chemistry, 231*, 259–275.

Carling, D. E. (1996). Grouping *Rhizoctonia solani* by hyphal anastomosis reaction. In S. Sneh, S. Jabaji-Hare, S. Neate, & G. Dijst (Eds.), *Rhizoctonia species: Taxonomy, molecular biology, ecology, pathology, and disease control* (pp. 37–47). Dordrecht: Kluwer Academic Publishers.

Carling, D. E., Baird, R. E., Gitaitis, R. D., Brainard, K. A., & Kuninaga, S. (2002). Characterization of AG-13, a newly reported anastomosis group of *Rhizoctonia solani*. *Phytopathology, 92*, 893–899.

Carling, D. E., Liner, R. H., & Westphale, P. C. (1989). Symptoms signs and yield reduction associated with Rhizoctonia disease of potato induced by tuberborne inoculum of *Rhizoctonia solani* AG-3. *American Potato Journal, 66*, 693–701.

Castrillo, J. I., Hayes, A., Mohammed, S., Gaskell, S. J., & Oliver, S. G. (2003). An optimized protocol for metabolome analysis in yeast using direct infusion electrospray mass spectrometry. *Phytochemistry, 62*, 929–937.

Chet, I., & Henis, Y. (1975). Sclerotial morphogenesis in fungi. *Annual Review of Phytopathology, 13*, 169–192.

Christensen, D., Foged, C., Rosenkrands, I., Nielsen, H. M., Andersen, P., & Agger, E. M. (2007). Trehalose preserves DDA/TDB liposomes and their adjuvant effect during freeze-drying. *Biochimica et Biophysica Acta, 1768*, 2120–2129.

Defernez, M., & Colquhoun, I. J. (2003). Factors affecting the robustness of metabolite fingerprinting using ^{1}H NMR spectra. *Phytochemistry, 62*, 1009–1017.

Desbrosses, G. G., Kopka, J., & Udvardi, M. K. (2005). *Lotus japonicus* metabolic profiling. Development of gas chromatography mass spectrometry resources for the study of plant–microbe interactions. *Plant Physiology, 137*, 1302–1318.

Dunn, W. B. (2008). Current trends and future requirements for the mass spectrometric investigation of microbial, mammalian and plant metabolomes. *Physical Biology, 5*, 1–24.

Efron, B., & Gong, G. (1983). A leisurely look at the bootstrap, the Jack-knife, and cross-validation. *American Statistician, 37*, 36–48.

Eriksson, L., Johansson, E., Kettaneh-Wold, N., & Wold, S. (2001). *Multi- and megavariate data analysis, Principles and applications*. Umeå, Sweden: Umetrics Academy.

Fiehn, O., Kopka, J., Dormann, P., Altmann, T., Trethewey, R. N., & Willmitzer, L. (2000). Metabolite profiling for plant functional genomics. *Nature Biotechnology, 18*, 1157–1161.

Forgue, P., Halouska, S., Werth, M., Xu, K., Harris, S., & Powers, R. (2006). NMR metabolic profiling of *Aspergillus nidulans* to monitor drug and protein activity. *Journal of Proteome Research, 5*, 1916–1923.

Foster, A. J., Jenkinson, J. M., & Talbot, N. J. (2003). Trehalose synthesis and metabolism are required at different stages of plant infection by *Magnaporthe grisea*. *EMBO Journal, 22*, 225–235.

Frank, J. A., & Francis, S. K. (1976). The effect of a *Rhizoctonia solani* phytotoxin on potatoes. *Canadian Journal of Botany, 54*, 2536–2540.

Georgiou, C. D., & Petropoulou, K. P. (2001). Effect of the antioxidant ascorbic acid on sclerotial differentiation in *Rhizoctonia solani*. *Plant Pathology, 50*, 594–600.

Gottlieb, D., & Van Etten, J. L. (1966). Changes in fungi with age I. Chemical composition of *Rhizoctonia solani* and *Sclerotium bataticola*. *Journal of Bacteriology, 91*, 161–168.

Huang, H. C. (1983). Histology, amino acid leakage, and chemical composition of normal and abnormal sclerotia of *Sclerotinia sclerotiorum*. *Canadian Journal of Botany, 61*, 1443–1447.

Iacobellis, N. S., & DeVay, J. E. (1987). Studies on pathogenesis of *Rhizoctonia solani* in beans: An evaluation of the possible role of phenylacetic acid and its hydroxy derivatives as phytotoxins. *Physiological Plant Pathology, 30*, 421–432.

Iturriaga, G. (2008). The LEA proteins and trehalose loving couple: A step forward in anhydrobiotic engineering. *Biochemical Journal, 410*, e1–e2.

Jager, G., Velvis, H., Lamers, J. G., Mulder, A., & Roosjen, Js. (1991). Control of *Rhizoctonia solani* on potatoes by biological, chemical and integrated measures. *Potato Research, 34*, 269–284.

Krishnan, P., Kruger, N. J., & Ratcliffe, R. G. (2005). Metabolite fingerprinting and profiling in plants using NMR. *Journal of Experimental Botany, 56*, 255–265.

Lucini, E. I., Zunino, M. P., López, M. L., & Zygadlo, J. A. (2006). Effect of monoterpenes on lipid composition and sclerotial development of *Sclerotium cepivorum* Berk. *Journal of Phytopathology, 154*, 441–446.

Mandava, N. B., Orellana, R. G., Warthen, J. D., Jr., et al. (1980). Phytotoxins in *Rhizoctonia solani*: Isolation and biological activity of m-hydroxy- and m-methoxyphenylacetic acids. *Journal of Agricultural and Food Chemistry, 28*, 71–75.

Manners, J. M., Maclean, D. J., & Scott, K. J. (1984). Hexitols as major intermediates of glucose assimilation by mycelium of *Puccinia graminis*. *Archives of Microbiology, 139*, 158–161.

Mas, S., Villas-Boas, S. G., Hansen, M. E., Akesson, M., & Nielsen, J. (2007). A comparison of direct infusion MS and GC-MS for metabolic footprinting of yeast mutants. *Biotechnology and Bioengineering, 96*, 1014–1022.

Mohler, R. E., Dombek, K. M., Hoggard, J. C., Pierce, K. M., Young, E. T., & Synovec, R. E. (2007). Comprehensive analysis of yeast metabolite GCxGC-TOFMS data: Combining discovery-mode and deconvolution chemometric software. *Analyst, 132*, 756–767.

Noverr, M. C., & Huffnagle, G. B. (2004). Regulation of *Candida albicans* morphogenesis by fatty acid metabolites. *Infection and Immunity, 72*, 6206–6210.

Ott, K. H., Aranibar, N., Singh, B., & Stockton, G. W. (2003). Metabonomics classifies pathways affected by bioactive compounds. Artificial neural network classification of NMR spectra of plant extracts. *Phytochemistry, 62*, 971–985.

Parmeter, J. R., Jr, & Whitney, H. S. (1970). Taxonomy and nomenclature of the imperfect state. In J. R. Parmeter Jr (Ed.), *Rhizoctonia solani, biology and pathology* (pp. 7–19). California: University of California Press.

Patsoukis, N., & Georgiou, C. D. (2007). Effect of glutathione biosynthesis-related modulators on the thiol redox state enzymes and on sclerotial differentiation of filamentous phytopathogenic fungi. *Mycopathologia, 163*, 335–347.

Priyatmojo, A., Yamauchi, R., Carling, D. E., Kageyama, K., & Hyakumachi, M. (2002). Differentiation of three varieties of *Rhizoctonia circinata*; var. circinata, var. oryzae and var. zeae on the basis of cellular fatty acid composition. *Journal of Phytopathology, 150*, 1–5.

Ratcliffe, R. G., & Shachar-Hill, Y. (2001). Probing plant metabolism with NMR. *Annual Review of Plant Physiology and Plant Molecular Biology, 52*, 499–526.

Secor, G. A., & Gudmestad, N. C. (1999). Managing fungal diseases of potato. *Canadian Journal of Plant Pathology, 21*, 213–221.

Siddiqui, I. A., & Shaukat, S. S. (2005). Phenylacetic acid-producing *Rhizoctonia solani* represses the biosynthesis of nematicidal compounds in vitro and influences biocontrol of *Meloidogyne incognita* in tomato by *Pseudomonas fluorescens* strain CHA0 and its GM derivatives. *Journal of Applied Microbiology, 98*, 43–55.

Smedsgaard, J., & Nielsen, J. (2004). Metabolite profiling of fungi and yeast: from phenotype to metabolome by MS and informatics. *Journal of Experimental Botany, 56*, 273–286.

Sorrell, T. C., Wright, L. C., Malik, R., & Himmelreich, U. (2006). Application of proton nuclear magnetic resonance spectroscopy to the study of *Cryptococcus* and cryptococcosis. *FEMS Yeast Research, 6*, 558–566.

Sumner, D. R. (1996). Sclerotia formation by Rhizoctonia species and their survival. In B. Sneh, S. Jabaji-Hare, S. Neate, & G. Dijst (Eds.), *Rhizoctonia species: Taxonomy, molecular biology, ecology, pathology and disease control* (pp. 207–217). The Netherlands: Kluwer Academic Publishers.

Takahashi, H., Kai, K., Shinbo, Y., et al. (2008). Metabolomics approach for determining growth-specific metabolites based on Fourier transform ion cyclotron resonance mass spectrometry. *Analytical and Bioanalytical Chemistry, 391*, 2769–2782.

Van den Boogert, P. H. J. F., & Luttikholt, A. J. G. (2004). Compatible biological and chemical control systems for *Rhizoctonia solani* in potato. *European Journal of Plant Pathology, 110*, 111–118.

Ward, J. L., Harris, C., Lewis, J., & Beale, M. H. (2003). Assessment of ^{1}H NMR spectroscopy and multivariate analysis as a technique for metabolite fingerprinting of *Arabidopsis thaliana*. *Phytochemistry, 62*, 949–957.

Yu, J.-H., & Keller, N. (2005). Regulation of secondary metabolism in filamentous fungi. *Annual Review of Phytopathology, 43*, 437–458.

Zervoudakis, G., Tairis, N., Salahas, G., & Georgiou, C. D. (2003). β-carotene production and sclerotial differentiation in *Sclerotinia minor*. *Mycological Research, 107*, 624–631.